

# Circumstellar envelopes and their descendents

Javier Alcolea<sup>1</sup>, Valentín Bujarrabal<sup>1</sup>, Jean-François Desmurs<sup>1</sup>, José Francisco Gómez<sup>2</sup>, and Carmen Sánchez Contreras<sup>3</sup>

<sup>1</sup>Observatorio Astronómico Nacional, IGN. <sup>2</sup>Instituto de Astrofísica de Andalucía, CSIC.

<sup>3</sup>Centro de Astrobiología, INTA-CSIC.

## Abstract

Copious mass-loss in thermally pulsating evolved stars is responsible for the formation of circumstellar envelopes and planetary nebulae, which in turn constitute the major source for the galactic enrichment in dust and light elements. The detailed study of these envelopes and nebulae requires normally both high angular resolution and sensitivity, as these sources are typically at distances of several hundreds of pc. These needs will be fully met at cm-wavelengths by the SKA. This instrument will significantly contribute to the better knowledge of these sources in many fundamental aspects [14]. Such as the compact ionized cores of nascent planetary nebulae (observations of radio continuum and radio-recombination lines); the cool outer parts of their envelopes (observations of HI, CH and OH); or the onset of the bipolarity in the pre-planetary nebulae phase, and its possible relationship with magnetic dynamos (observations of OH masers and their Zeeman splitting).

## 1 Introduction

The thermally-pulsating asymptotic giant branch (TP-AGB) is one the latest stages of evolution of stars with masses  $\sim 1 - 8 M_{\odot}$ . At this point, these asymptotic red giant stars (aRGs) experience a huge mass-loss ( $\sim 10^{-8} - 10^{-4} M_{\odot} \text{ yr}^{-1}$ ) that determines their ulterior evolution. These mass ejections lead to the formation of dense circumstellar envelopes (CSEs), with total masses up to some  $M_{\odot}$ , that gently expand into the interstellar medium (ISM). These CSEs will later transform into planetary nebulae (PNe), when the host star, denuded from its mantle as a result of the mass-loss, gets hot enough ( $\gtrsim 25,000 \text{ K}$ ) in its way to the white dwarf phase and ionizes its surroundings. Very similar mass-loss processes also occur in the heavier counterparts of TP-AGB stars, the red super-giants (RSGs) and yellow hyper-giants (YHGs), diminishing the final mass of the core-collapse supernova and constituting the circumstellar environment the supernova blast will run into. In addition to this, CSEs of both aRGs and RSGs/YHGs constitute the most important source of dust and light metals enrichment in the galaxy. Yet, we are still far from understanding how these mass-loss processes occur. For

example, we still do not have a reliable analytical mass-loss rate formula to use in population synthesis models, and we are far from understanding the extreme latest mass-loss event which results in the birth and shaping of PNe.

### 1.1 The neutral atomic gas: observations of the HI 21-cm line

CSEs are formed by gas and dust particles, with typical gas-to-dust mass ratios of a few hundreds. The most abundant constituent of the gas phase is obviously hydrogen, that is usually found in molecular ( $\text{H}_2$ ) or neutral atomic (HI) form depending on whether the temperature of the central star is less or more than 2500 K respectively [8].  $\text{H}_2$  rotational and ro-vibrational lines are strongly forbidden, and can only be observed in the IR from hot gas or ionized regions close to the star, or in the presence of strong shocks, and therefore it can not be used to trace the cool outer parts of the CSEs [11]. The study of these circumstellar regions is usually done by means of the observation of low-excitation rotational lines of other molecules, mainly CO. However, CO (and other molecules too) can only trace the mass-loss history of the stars up to its photo-dissociation radius, 0.1 pc at most, which means only 10 000 yr back in time, about 10% of the whole TP-AGB phase duration. Indeed, we know that CSEs can be much larger,  $\sim 0.1$ –to 1.0 pc, as shown by the IR emission of the circumstellar cold dust [13]. Unfortunately, dust emission does not provide any information on the kinematics (i.e., mass-loss rates can not be computed), and total mass estimations are model dependent (grain composition and size, gas-to-dust ratio, etc.). These outermost layers are very interesting, as they are where both circumstellar and interstellar media interact, sometimes resulting in the formation of very extended bows and/or cometary tails of shocked excited gas [16].

These very outer parts of CSEs can in principle be probed by observing the 21-cm (1420 MHz) hyperfine structure transition of HI. However, this is a very difficult task for the current instrumentation, because of the weakness of this emission in CSEs and the strong contamination due to the ISM. Both problems can largely be circumvented by the SKA expected capabilities: the much higher sensitivity and the ability of performing high-fidelity mapping of structures over a wide range of spatial scales. Due to the present observational limitations, the existing observations of HI in CSEs are meagre, and sometimes difficult to interpret. Using the Nançay radio-telescope, the VLA, the GMRT, and the GBT, about a dozen sources have been detected in the 21-cm HI line [21, 7]. In some cases (e.g. IRC +10°216 and R Cas) there are still doubts that the detected signal is indeed of circumstellar origin and not due to ISM gas along the line of sight. However, in the cases of Ep Apr, *o* Cet, RC Cnc, Y Cvn, and RX Lep, the detections are clear and the estimated HI mass-loss rates are sometimes comparable to those inferred from CO. In particular, the case of *o* Cet is very interesting, as HI is detected in a extremely long ( $\sim 3$  pc) cometary tail also seen in X-rays [20]. This tail would consist of circumstellar gas stripped off as result of the motion of the star with respect to the local ISM. This could also be the case of RS Cnc and RX Lep.

In view of these few but promising results, it is expected that the revolutionary HI 21-cm line observations that SKA should provide, will open a new window for studying CSEs at large scales. This, in combination with other data, will give us a much complete view of the mass-loss history in evolved stars and its impact on the chemistry and dynamics of the ISM.

## 1.2 Thermal emission of light molecules: OH and CH $\Lambda$ -doubling lines

Molecules in CSEs and young-PNe (yPNe) are usually observed at mm- and submm-wavelengths. However, some key species can also be observed at lower frequencies. In particular, the CH and OH radicals have  $\Lambda$ -doublet transitions at cm-wavelengths. These molecules, which show widespread emission in both interstellar and circumstellar environments, are important carriers of abundant elements and thus constitute basic chemical ingredients.

OH is well known to display strong maser emission in several  $\Lambda$ -doubling lines at 18-cm, from the  $\Pi=3/2$   $J=3/2$  rotational ground level (see later). These lines must also show thermal (i.e. non maser) emission under certain conditions. The advantage of observing the thermal emission is that the interpretation of the results is more straightforward than for masers, and that it traces the overall structure and dynamics of the emitting nebula more directly. Of course, the disadvantage is that the lines are weaker by orders of magnitude. To date, such thermal lines have been only observed with single-dish telescopes, from very extended nebulae, and with very poor spatial resolution. The very high sensitivity of SKA should allow systematic observations of thermal emission of the four OH 18-cm lines. We expect these lines to be optically thick, and therefore, brightness temperatures of the order of the kinetic temperature in the OH emitting regions:  $\sim 100$  K or higher in both CSEs and in shocks propagating in young PNe [10, 3]. This results in line intensities detectable for the SKA, even at  $1''$  resolution, in reasonably short integration times.

CH, the counterpart of OH in C-rich environments [24], very often shows weak maser emission at 3.3 GHz, from the three  $\Lambda$ -doubling components of the ground rotational levels [2]. Because of the weak amplification, for CH we can just expect brightness levels over 50 K, even if population inversion is practically universal in this case. For this reason, high spatial resolution observations of CH are very rare, and most data have been obtained using single-dish radio-telescopes. However, the SKA sensitivity at 3.3 GHz, in units of brightness temperature, must be significantly higher than for the OH lines (about 4 times better). Therefore, the CH cm-wave lines should be detectable with SKA, with enough angular resolution for detailed mapping, in a large number of sources.

## 1.3 Ionized cores of pPNe: radio continuum and RRLs observations

PNe are ionized remnants of CSEs, but while the latter are roughly spherically symmetric, the former are mostly bipolar and often show most bizarre structures. The physical mechanisms responsible for this transformation is yet unknown, but it must be active in the very early stages of the evolution beyond the TP-AGB, the pre-planetary nebula (pPN) phase. Therefore, pPNe, and yPNe too, hold the key for understanding this complex and fast ( $\sim 1000$  yr) nebular evolution. Studies of pPNe support the idea that the multiple lobes and high-velocities observed in pPNe and PNe are produced by the interaction of fast collimated winds (jets) with the spherical and slowly expanding CSE. However, this jet+CSE two-wind interaction scenario remains unconfirmed by the direct observation of the jets themselves, and of the central nebular regions from where these jets should be launched (a few 100 AU). Studying these central regions is difficult due to their small angular extent (sub-arcsec.)

and because they are heavily obscured by dense central circumstellar dust layers. Progress requires sensitive high-angular resolution observations at long wavelengths, which could be swimmingly provided by SKA in the future.

Typically, central stars of PNe start ionizing their envelopes when they reach a B-type spectral classification. Optical spectroscopic observations of pPNe and yPNe have revealed the presence of widespread broad ( $\sim 100\text{--}1000\text{ km s}^{-1}$ )  $\text{H}\alpha$  emission, often with blue-shifted absorption features (P Cyg profiles) produced at their nuclei [27]. Surprisingly,  $\text{H}\alpha$  emission is also found in some pPNe with much cooler central stars, suggesting the presence shocks in the stellar vicinity, which could be linked to on-going jets sculpting the inner regions of the old CSE, or to mass-accretion by a compact companion. Due to the large dust opacity of these regions in the visible, in most cases these nuclei can only be indirectly observed via their dust reflected light. This situation not only makes the observations more difficult, but also complicates the interpretation of the observed profiles [26]. These central ionized regions of pPNe and yPNe are visible through radio-continuum and radio-recombination line (RRL) emission at long wavelengths, which have the key advantage of being dust-extinction free.

In contrast to more evolved PNe, continuum flux measurements at wavelengths beyond  $\sim 1\text{ cm}$  are lacking for the vast majority of pPNe and yPNe. This is because at these long-wavelengths their compact, just emerging ionized cores are very weak emitters. Typically, reliable detections in pPNe/yPNe would require sensitivities better than  $\sim 0.01\text{ mJy}$ , which are difficult to achieve with the current facilities in reasonable observing times. However, it is at centimetre (and longer) wavelengths where the thermal bremsstrahlung (free-free) radiation, produced by these nascent ionized cores, becomes observable and much stronger than any possible contamination from thermal cold dust emission. The unprecedented capabilities of the SKA, which will routinely reach sub- $\mu\text{Jy}$  sensitivities at sub-arcsecond resolution, should allow to carry out sensitive radio continuum imaging observations of pPNe/yPNe. Resolving the morphology of the central ionized regions, down to  $\approx 1\text{--}100\text{ AU}$  spatial scales, holds the promise for unveiling some of the pivotal structures postulated by most PNe shaping theories. The SKA could perform time-series imaging of the expansion and development of these central HII regions, as well as of the changes in the shock activity. The SKA could also provide maps of the free-free emission turnover frequency, and thus maps of the emission measure. This can be used to deduce the spatial distribution of the electron density, and to estimate the present-day (post-AGB) mass-loss rate, a long sought key parameter in the post-AGB evolution. Imaging the continuum at long wavelengths where the free-free emission becomes optically thick, will provide a measure of the electron temperature throughout the nebulae [18]. Radio continuum maps can also be compared with  $\text{H}\alpha$  images at optical wavelengths, to obtain dust extinction maps of these objects [30]. Mapping the spectral index variation across the nebulae will show whether other emission mechanisms, such as synchrotron radiation from magnetically collimated jets [23], whose contribution to the radio continuum flux cannot be excluded, are present at these early post-AGB phases.

Observations of RRLs are challenging, especially in the cm- to m-wavelength range, where these lines are extremely weak in comparison to the continuum level (typically  $\sim 1\%$ ). To date, mm- and cm-wavelength RRLs studies have been carried out for some of the best-known and most luminous evolved PNe [1, 30], but this field remains largely unexplored for

pPNe and yPNe. RRLs have only been sought and detected in the mm-wavelength range towards the C-rich pPN CRL 618 [17]. In the frequency range covered by SKA there are hundreds of hydrogen recombination lines ( $Hn\alpha$ , with  $n > 90$ ) that are ideal tools to image the structure, physical conditions (electron temperature and density), and kinematics of the central ionized regions of pPNe/yPNe. These low-frequency transitions, although much weaker than those in the mn-wave range, are particularly well suited to study the current, fast but tenuous ( $< 100 \text{ cm}^{-3}$ ) post-AGB winds that fill in the central cavities inside CSEs that result from the abrupt decrease of the mass-loss rate (by several orders of magnitude), after the central star departs from the TP-AGB. RRLs studies with SKA will fully complement analogous observations at higher frequencies (e.g. with ALMA), which are better probes of the inner and denser ( $\sim 10^5\text{--}10^7 \text{ cm}^{-3}$ ) environments. RRLs arising from other elements, such as He and C, can also be observed simultaneously to the hydrogen RRLs, providing a direct measurement of the chemical composition of the material ejected in the late-AGB and early post-AGB phases. We are confident that multi-frequency RRLs observations, with the exceptional high-sensitivity and high-angular resolution imaging capabilities of SKA, will certainly produce significant new insights into the structure, dynamics, and physicochemical conditions of the central regions of pPNe/yPNe, and will help in addressing the problem of the formation and shaping of post-AGB nebulae.

#### 1.4 Maser emission from CSEs and beyond

Maser emission is often observed in the CSEs of aRGs and RSGs. In particular, sources in which oxygen is more abundant than carbon, O-rich CSEs, can show strong maser emission in several lines of silicon monoxide (SiO), water vapour ( $\text{H}_2\text{O}$ ) and hydroxyl (OH). These emissions have been widely used to characterize the geometry and velocity field of these envelopes at high angular resolution.

OH masers are typically observed in the  $\Lambda$ -doubling hyperfine transitions at 1.6–1.7 GHz, from the  $\Pi=3/2$   $J=3/2$  ground-rotational states. These lines have been observed towards hundreds of CSEs and some PNe. Maser emission from OH hyperfine transitions in vibrationally excited states is also very common in star-forming regions. On the contrary, the lines from the first vibrationally excited state at 6 GHz are either undetected or extremely rare and weak in evolved stars: just a few possible detections have been reported both in CSEs, NML Cyg and AU Gem, and in yPNe, Vy 2\_2 and K 3-35 [4]. All these studies will greatly benefit of the advent of the SKA, as its frequency coverage will embrace not only the ground-rotational lines at 1.6–1.7 GHz, but also excited lines at 4.7, 6, and 13 GHz.

One of the possible key programs for the SKA, due to its high sensitivity, will be to perform deep maser surveys. In particular, OH surveys promise to be very fruitful, not only to detect new masers much farther away (beyond galactic center, or towards near galaxies such the Magellanic Clouds, M 31, M 33, etc.), but also to extend the searches towards much weaker luminosities, and thus making possible the detection of possible new excited masers. The increase in number of known OH masers will be especially interesting for dynamical studies. Using phase referencing techniques, it is possible to determine distances with a high accuracy, not only for stars in our local galactic arm, but also for the Galactic Center, and

even nearby galaxies. This will result in a much better sampling of the rotation curve of our galaxy, as well as a new trigonometric parallax distances to Local Group galaxies.

The widespread maser emission characteristic of CSEs of TP-AGB stars disappears shortly after the end of this phase, when the mass-loss rate drops dramatically, from  $\simeq 10^{-4}$  to  $10^{-7} M_{\odot} \text{ yr}^{-1}$  [29]. After the end of the TP-AGB, the survival time-scales are roughly  $\simeq 10, 100,$  and  $1000$  years for SiO, H<sub>2</sub>O, and OH masers, respectively [9, 15]. Therefore, maser emission is less likely to be found as the star further evolves into the post-AGB phase, and it is extremely rare in PNe. However, despite their lower detection rates, maser emission can provide key insights on the collimated mass-loss processes during these post-AGB phases, which determine how PNe are shaped.

The spectra of OH maser emission in CSEs typically shows two well-defined peaks, with separations  $\simeq 30 \text{ km s}^{-1}$  [28], corresponding to the approaching and receding sides of the circumstellar envelope, which is expanding with a roughly spherical symmetry at a constant velocity. However, the post-AGB and early PN phases are characterized by mass-loss in the form of fast collimated jets, and maser emission from these objects shows a clear departure from the double-peaked pattern: an easily recognizable hallmark of non-spherical mass-loss [5]. Important maser-emitting objects in this phase are the so called *water fountains* (WFs) [12, 6]. These are evolved stars with H<sub>2</sub>O maser emission tracing high-velocity ( $> 80 \text{ km s}^{-1}$ ) jets of very short dynamical ages ( $< 100 \text{ yr}$ ). They could represent one of the first manifestations or collimated mass-loss in evolved objects and thus, are key targets to understand the subsequent shaping of PNe. While studies of WFs normally focus on their H<sub>2</sub>O maser emission, they also show OH emission tracing jets [25]. SKA observations of OH masers in WFs and other post-AGB stars will allow us to study their jet morphology with unprecedented detail. Using SKA1-mid, in one hour of observing time and a velocity resolution of  $0.2 \text{ km s}^{-1}$ , the relative positional accuracy between two different OH maser spots at the level of  $0.5 \text{ Jy}$  will be  $\simeq 150$  micro-arcsec. This means that we can study maser distributions of  $\simeq 1 \text{ AU}$  for sources as distant as the Galactic center. This level of precision, which is impossible to obtain with current radio interferometers, will be key to understand where and how mass-loss is produced in these evolved stars. Moreover, observations in different epochs would give us the opportunity to measure proper motions. Therefore, it will be possible to obtain, both the spatial distribution and the 3-dimensional velocity structure of masers in these objects. With this, we could study the launching location and the mass-loss history of jets (e.g., whether they are continuous or explosive events). This can be related to the physical origin of the jets, in particular whether they are powered by accretion disks [19] or via energy release in magnetic dynamos [22].

In addition, because of its non zero electronic angular momentum, the OH radical is a natural magnetometer. By measuring the intensity of the Zeeman splitting effect, we can determine the value of the magnetic field along the line of sight,  $B_{\parallel}$ , in the regions where the maser emission arises. The role of magnetic fields in evolved stars has not been explored in detail, though it must influence the dust formation process, the launching of circumstellar winds, and obviously provide information on the magnetic properties of the star. Measuring the magnetic field in these OH-emitting regions in a large number of sources will provide invaluable information on these issues, but it can only be done with SKA capabilities.

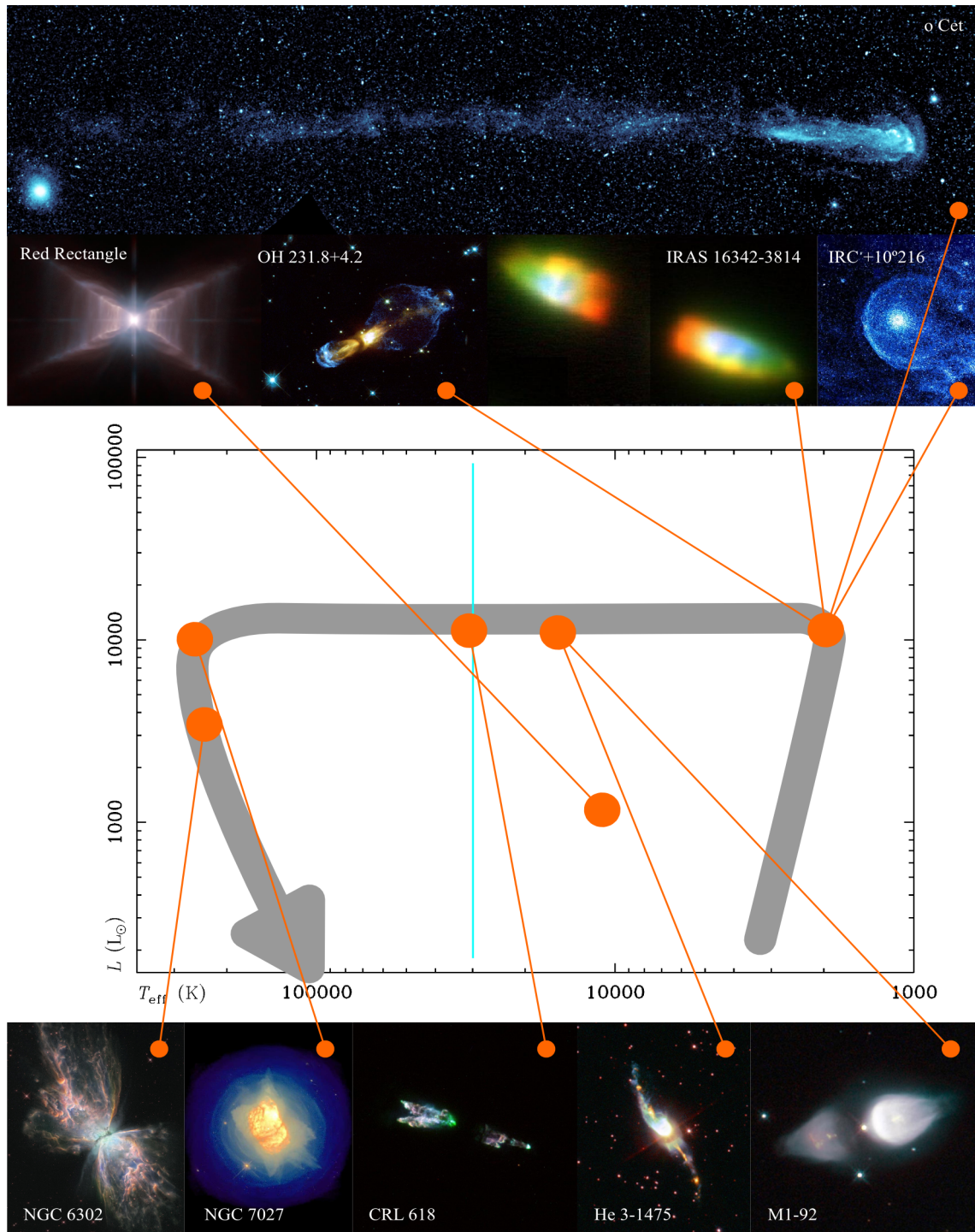


Figure 1: HR-diagram of the late evolution of intermediate mass stars ( $\sim 1 - 8 M_{\odot}$ ), including the location of some of the sources mentioned in the text, as well as images of their envelopes and nebulae.

## Acknowledgments

This work has been financially supported by MINECO (Spain) grants CSD 2009-00038, AYA 2009-07304, AYA 2011-30228-C03-01, AYA 2012-32032, FIS 2012-32096, and AYA 2014-57369-C3-3-P.

## References

- [1] Bachiller, R., Huggins, P. J., Martín-Pintado, J., Cox, P., 1992, *A&A*, 256, 231
- [2] Bujarrabal, V., Salinas, F., Gonzalo, I., 1984, *ApJ*, 285, 312
- [3] Bujarrabal, V., Alcolea, J., Soria-Ruiz, R., et al., 2012, *A&A*, 537, AA8
- [4] Desmurs, J.-F., Baudry, A., Sivagnanam, P., et al., 2010, *A&A*, 520, 45
- [5] Deacon, R. M., Chapman, J. M., Green, A. J., 2004, *ApJS*, 155, 595
- [6] Desmurs, J.-F., 2012, *IAU Symposium*, 287, 217
- [7] Gérard, E., Le Bertre, T., Libert, Y., 2011, *SF2A Conf.*, 419
- [8] Galssgold, A. E., Huggins, P. J., *MNRAS*, 203, 517
- [9] Gómez, Y., Moran, J. M., Rodríguez, L. F., 1990, *RevMexAA*, 20, 55
- [10] Goldreich, P., Scoville, N., 1976, *ApJ*, 205, 144
- [11] Habart, E., Walmsley, M., Verstraete, L., et al, 2005, *SSR* 119, 71
- [12] Imai, H., 2007, *IAU Symposium*, 242, 279
- [13] Izumiura, H., Hashimoto, O., Kawara K., et al., 1996, *A&A*, 315, L221
- [14] Marvel, K., 2004, *NewAR* 48, 1349
- [15] Lewis, B. M., 1989, *ApJ*, 338, 234
- [16] Martin, D. C., Seibert, M., Neill, J. D., et al., 2007, *Nature*, 448, 780
- [17] Martín-Pintado, J., Bujarrabal, V., Bachiller, et al., 1988, *A&A*, 197, L15
- [18] Martín-Pintado, J., Gaume, R., Bachiller, R., Johnson, K., 1993, *ApJ*, 419, 725
- [19] Mastrodemos, N., Morris, M., 1998, *ApJ*, 497, 303
- [20] Matthews, L. D., Libert, Y., Gérard, E., et al., 2008, *ApJ*, 684, 603
- [21] Matthews, L. D., Le Bertre, T., Gérard, E., Johnson, M. C., 2013, *AJ*, 145, 97
- [22] Nordhaus, J., Blackman, E. G., 2006, *MNRAS*, 370, 2004
- [23] Pérez-Sánchez, A. F., Vlemmings, W. H. T., Tafoya, D., et al., 2013, *MNRAS*, 436, L79
- [24] Rydbeck, O. E. H., Kollberg, E., Hjalmanson, A., et al., 1976, *ApJSS*, 31, 333
- [25] Sahai, R., te Lintel Hekkert, P., Morris, M., et al., 1999, *ApJL*, 514, L115
- [26] Sánchez Contreras, C., Sahai, R., 2001, *ApJ*, 553, L173
- [27] Sánchez Contreras, C., Sahai, R., Gil de Paz, A., Goodrich, R., 2008, *ApJS*, 179, 166
- [28] Sevenster, M. N., Chapman, J. M., Habing, et al., 1997, *A&AS*, 122, 79
- [29] Vassiliadis, E., Wood, P. R., 1994, *ApJS*, 92, 125
- [30] Vázquez, R., Torrelles, J. M., Rodríguez, L. F., et al., 1999, *ApJ*, 515, 633